Comparative transcriptional profiling of the lung reveals shared and distinct features of *Streptococcus pneumoniae* and influenza A virus infection

Simone Rosseau,[1] Andreas Hocke,[1] Hans Mollenkopf,[2] Bernd Schmeck,[1] Norbert Suttorp,[1] Stefan H. E. Kaufmann[3] and Jens Zerrahn[3,4]

[1]*Department of Internal Medicine, Infectious Diseases and Respiratory Medicine, Charité–Universitätsmedizin Berlin,* [2]*Core Facility Microarrays, and* [3]*Department of Immunology, Max Planck Institute for Infection Biology, Berlin, Germany*

doi:10.1111/j.1365-2567.2006.02514.x
Received 12 July 2006; revised 6 October 2006; accepted 6 October 2006.
Present address: [4]Institute of Clinical Pharmacology Parexel International GmbH, Spandauer Damm 130, 14050 Berlin, Germany.
Correspondence: Dr S. H. E. Kaufmann, Department of Immunology, Max Planck Institute for Infection Biology, Charitéplatz 1, 10117 Berlin, Germany.
Email: kaufmann@MPIIB-Berlin.MPG.DE
Senior author: S. H. E. Kaufmann
This article has an online supplement.

Summary

Pneumonia is the most common cause of death from infectious disease in the western hemisphere. Pathophysiological and protective processes are initiated by pattern recognition of microbial structures. To provide the molecular framework for a better understanding of processes relevant to host defence in pneumonia, we performed pulmonary transcriptome analysis in mice infected with the major bacterial and viral agents of community-acquired pneumonia, *Streptococcus pneumoniae* and influenza A virus. We detected differential expression of 1300 genes after infection with either pathogen. Of these, approximately 36% or 30% were specific for pneumococcal or influenza infection, respectively, yielding pathogen-specific as well as shared inflammatory transcriptional signatures. These results not only reveal a differential response on the cytokine and chemokine levels but also emphasize the important role of genes implicated in regulation and fine tuning of inflammation. As one, albeit unexpected, key feature of pneumococcal pneumonia we discovered down-regulation of B-cell responses, probably reflecting a pneumococcal virulence strategy. The pathophysiological consequences of influenza A virus infection were reflected by the emerging protective T-cell response and differential induction of genes involved in tissue regeneration and proliferation. These data provide new insights into pathogenesis of the most common forms of pneumonia, highlighting the value of transcriptional profiling for the elucidation of underlying mechanisms.

Keywords: influenza; lung; pneumococci; pneumonia; transcriptome

Introduction

Streptococcus pneumoniae and influenza virus are the most important agents of community-acquired pneumonia with substantial morbidity and mortality worldwide.[1–3] As a further complication, influenza virus infection frequently paves the way for pneumococcal infection so exacerbating the impact of pandemic influenza.[4] In addition to microbial virulence factors, detrimental aspects of the host response against both infections have been increasingly recognized as contributing significantly to the fatal outcome of infection.[5–7] Deeper understanding of beneficial or detrimental pulmonary immune mechanisms can provide guidelines for rational improvement of current diagnostic and therapeutic regimens.

Global transcriptional profiling is a powerful approach for analysing the host response during the course of infection, providing insights into unique parameters determined by the nature of the pathogen and the mode of infection. *In vitro* studies using defined cell lines are suggestive of molecular aspects of the pro-inflammatory defence response elicited by *S. pneumoniae* or influenza virus.[8] However, in infected target organs, such as the lung in the case of pneumonia, it is the complex cellular interplay of immune as well as non-immune cells that determines the response on the molecular level, which is in part reflected by differential gene expression profiles. Although less discriminative at the cellular level, the potency of global transcriptome analysis of whole infected organs rests in the provision of a molecular framework as

Abbreviations: PIR, paired immunoglobulin-like receptor; TREM, triggering receptors expressed on myeloid cells.

the rational basis for a comprehensive understanding of underlying processes, guiding further elucidation of specific and general aspects of the host response.

In this study we compared the transcriptional signatures of pneumococcal pneumonia with those of an extensive inflammation induced by influenza A virus infection in mouse lungs. This comparative approach revealed a partial transcriptional signature overlap identifying genes that are common to the immune response against both pathogens, reflecting aspects of a general inflammatory response to pulmonary infection. In addition, we found transcriptional signatures that were specific for either pneumococci or influenza A virus, thereby reflecting the distinct nature of the pathogens and the courses of infection.

Materials and methods

Murine pneumonia models

Female C57BL/6 mice (8–12 weeks, 18–21 g; Charles River, Sulzfeld, Germany) were used for all experiments. Experiments were approved by local authorities (LAGetSi Berlin) and performed under specific pathogen-free conditions. For the induction of pneumococcal pneumonia, anaesthetized mice were transnasally inoculated with 5×10^6 colony-forming units of *S. pneumoniae* serotype 3 (NCTC7978) in 20 μl phosphate-buffered saline (PBS) as described previously.[9] Control mice received 20 μl sterile PBS. Infections with influenza A virus strain HKx31 (H3N2) were performed as described elsewhere.[10] Animals were intranasally infected with 360 haemagglutinating units in 30 μl allantoic fluid. Mock infections were performed with virus-free allantoic fluid.

Lung cell analysis and pulmonary bacterial load

At the indicated time-points after pneumococcal infection, lung leucocytes were prepared as described previously.[11] Blood was collected by cardiac puncture, and mononuclear cells were enriched from liver and spleen by filtration through 70-μm cell strainers (BD Biosciences, San Jose, CA) after erythrocyte lysis. Blood leucocyte counts were performed using BD TruCount©, and cells from organ specimens were counted on a haemocytometer. Flow cytometric analysis was performed on a FACS Calibur (Becton Dickinson, Franklin Lakes, NJ) after staining with CD45 PerCP (pan-leucocytes; clone 145-2C11, PharMingen, San Diego, CA), Gr-1 PE (neutrophil granulocytes; clone RB6-8C5, Miltenyi Biotec, Bergisch Gladbach, Germany), and CD19-APC (B cells; clone 1D3, Pharmingen). For histological analysis, lungs were flushed via the pulmonary artery with saline, transtracheally instilled with TissueTek OCT compound (Plano, Wetzlar, Germany), and frozen in liquid nitrogen. Ten-micrometre sections were cut from lung tissue blocks using a cryostat HM560 (Microm International, Walldorf, Germany). Histopathological assessment was performed on slides stained with haematoxylin & eosin. For quantification of bacterial loads, lungs were flushed via the pulmonary artery with sterile saline and homogenized. Serial dilutions of lung samples were plated on blood agar, and incubated at 37° for 16 hr before colonies were counted.

Preparation of total RNA from lungs

Mice ($n = 3$ per group) were killed at the indicated time-points, lungs were flushed via the pulmonary artery with sterile saline, and total RNA was prepared with 1 ml TRIzol (Invitrogen, Karlsruhe, Germany) per lung using an Ultraturrax T8 S8N-8G (IKA, Staufen, Germany). Homogenized aliquots were shock-frozen, stored at −70°, pooled after thawing, and processed for total RNA isolation as described by the manufacturer and purified using RNeasy (Qiagen, Hilden, Germany). RNA integrity and concentration analyses were performed with a Bioanalyser 2100 (Agilent Technologies, Palo Alto, CA).

DNA oligo microarrays

Two-colour microarrays were purchased from Agilent Technologies (Palo Alto, CA). They were manufactured using *in situ* SurePrint technology in 60-mer oligonucleotide format with a custom design (AMADID 010646), covering 8014 genes with a preference for immunological relevance. Labelling of RNA for hybridization was performed using the fluorescent linear amplification kit from Agilent Technologies according to the supplier's instructions. Briefly, 4 μg total RNA was reverse transcribed with an oligo-dT-T7 promoter primer and MMLV-RT. Second-strand synthesis was carried out with random hexamers. Fluorescent antisense cRNA was synthesized with either cyanine 3-CTP or cyanine 5-CTP and T7 polymerase. Purified products were quantified as absorbance at 552 nm ($A_{552\ nm}$) for cyanine 3-CTP and $A_{650\ nm}$ for cyanine 5-CTP. Before hybridization, 1·25 μg of each labelled cRNA was fragmented, mixed with control targets and with hybridization buffer according to the supplier's protocol (Agilent Technologies). Hybridizations were performed at 60° for 17 hr. Slides were washed according to the manufacturer's protocol and arrays were scanned at 5-μm resolution using a DNA microarray laser scanner (Agilent Technologies). Features were extracted from raw image data using the Agilent Technologies image analysis software (G2567AA Feature Extraction Software, Version A6·1.1·1) and default settings. A local background subtraction was applied. The arrays were normalized using rank consistency filtering of normalization feature selection, together with a combined linear and LOWESS curve fitting method. Ratios were calculated by the most conservative estimate between a universal error model and

propagated error. Data analysis was performed using the Rosetta Inpharmatics (Seattle, WA) RESOLVER software package BUILD 3·2.2. Ratio profiles were generated from raw scan data using a processing pipeline, which includes pre-processing (FEATURE EXTRACTION) and post-processing (ROSETTA RESOLVER) of data, and error model adjustments to the raw scan data. Ratio profiles were combined in an error-weighted fashion by RESOLVER to create ratio experiments. To compensate for dye-specific effects, and to ensure validity of the data, a colour-swap analysis (fluorescence reversal) was performed. Expression patterns were identified using stringent analysis criteria of two-fold expression cut-offs of the ratio experiments and an anti-correlation of the dye-reversal ratio hybridizations. Anti-correlation was determined by using the 'compare function' to compare two-colour-swap dye-reversal hybridizations and to decide how similar or dissimilar they were. In this way, only anti-correlated spots that were red on one array and green on the other, and vice versa, were selected. By combining the less than two-fold and the anti-correlation criteria, we filtered out data-points with low *P*-values, rendering the analysis highly robust and reproducible. After applying this strategy, all valid data-points had an error-weighted *P*-value $< 0{\cdot}01$. In addition, by using this strategy data selection was independent of the error models implemented in the Rosetta RESOLVER system.

Quantitative polymerase chain reaction analysis

Assorted genes exhibiting a more than two-fold difference of expression in microarray analysis were forwarded to quantitative polymerase chain reaction (PCR). For real-time quantitative PCR, total RNA was reverse transcribed using random hexamers (Pharmacia Biotech, Uppsala, Sweden) and Superscript II reverse transcriptase (Invitrogen) according to the recommendations of the manufacturer. SYBR Green (Applied Biosystems; Foster City, CA) uptake in double-stranded DNA was measured using an ABI PRISM 7000 thermocycler (Applied Biosystems) according to the manufacturer's instructions. The amplification primer pairs were designed with the ABI PRISM PRIMER EXPRESS Version 2·0.0 software (Applied Biosystems). Glyceraldehyde 3-phosphate dehydrogenase (GAPDH) and β-actin-specific cDNA amplifications were used as controls and GAPDH was used for subsequent data normalization.

Results

Pneumococcal and influenza pneumonia in mice

Inflammatory cell influx into the lungs emerged 12 hr after pneumococcal infection (Fig. 1a) and consisted predominantly of neutrophils (Fig. 1b). Histological analyses revealed focal inflammation after 24 hr (data not shown),

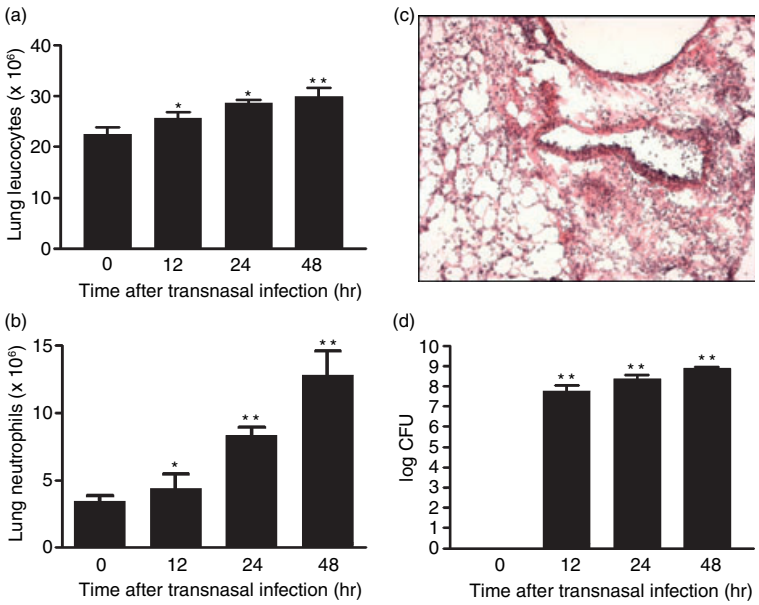

Figure 1. Inflammatory influx of leucocytes and granulocytes into the lung, histopathological consequence and lung bacterial burden after infection with *S. pneumoniae*. Mice transnasally infected with *S. pneumoniae* were killed 12 hr, 24 hr or 48 hr after infection. Control mice were challenged with 20 µl PBS, and killed after 48 hr. Lung cells were counted using a haemocytometer and leucocytes were further differentiated by FACS analysis of CD45 and Gr-1 expression. Data are presented as mean leucocyte (a) or granulocyte (b) numbers ± SEM, $^{*}P < 0{\cdot}05$, $^{**}P < 0{\cdot}01$ versus control, $n = 5$ each. The representative haematoxylin & eosin-stained cryosection of a blood-free mouse lung 48 hr after pneumococcal challenge confirms severe pneumonia (c). For the quantification of bacterial load, mice were killed 12 hr, 24 hr or 48 hr after infection. Blood-free lungs were homogenized, plated on blood agar and incubated at 37° for 16 hr before colony counting. Data are depicted as log colony forming units (CFU) ± SEM, $^{**}P < 0{\cdot}001$ versus control (non-infected mice), $n = 5$ each (d).

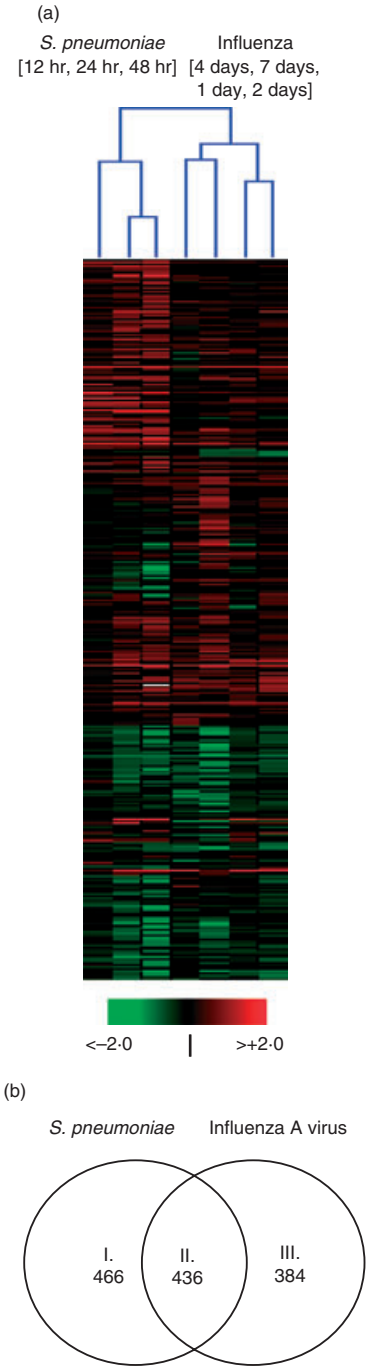

Figure 2. Pulmonary transcription signatures of mice infected with *S. pneumoniae* and influenza A virus. Different time-points of the *S. pneumoniae* and influenza A virus infections were analysed independently using the two criteria (i) more than two-fold differential expression of the combined colour-swap ratio profiles as ratio experiments and (ii) anti-correlation of the respective colour-swap ratio profiles. The set union of all analysis results comprised 1286 genes which were differentially expressed at least at one time-point during either infection. (a) This set union was used to generate a two-dimensional cluster containing a gene-level cluster and an experiment-level cluster in one graph by applying an agglomerative algorithm with the heuristic criterion 'average link' and the similarity measure 'Manhattan distance' for both classifications. The hierarchical structure of the time-points and infections is illustrated as a dendrogram while the fold change values are colour encoded with green for down-regulated genes, black for unregulated genes and red for up-regulated genes. (b) The set union of the different time-points of the *S. pneumoniae* infection comprised 902 genes and the set union of the different time-points of the influenza A virus infection included 820 genes. These two sets were compared and the Venn diagram shows the numbers of transcripts that were differentially expressed in a pathogen-specific or common manner.

and severe pneumonia was noted 48 hr after infection (Fig. 1c). Infected mice suffered from a dramatic increase in pulmonary bacterial load over time (Fig. 1d), and developed significant bacteraemia after 48 hr (data not shown). Respiratory influenza virus infection has been documented in several studies.[10,12,13] In essence, peak cellular infiltration occurs 7 days after infection and is predominated by lymphocytes; infectious virus is generally cleared 7 days after challenge.[10,12,13] Analysis of intracellular cytokine expression after restimulation with irradiated virus preparations[10] was employed for the determination of time-points for microarray analyses, covering the onset of infection and inflammation, as well as the full-blown clinical picture.

Transcriptional profiling: general results

We detected almost 1300 genes exhibiting differential relative levels of expression compared to respective mock-infected controls (Table S1). Of these, 466 genes were specific for infection with *S. pneumoniae*, and 384 genes were specific for influenza A virus infection, while 436 differentially expressed genes were common to infection with both pathogens (Fig. 2). The data discussed in this publication have been deposited in NCBIs Gene Expression Omnibus (GEO, http://www.ncbi.nlm.nih.gov/geo/) and are accessible through GEO Series accession number GSE5289. Microarray data were generated from pools of RNA derived from three individual mice as biological replicates and two technical replicates carried out as colour-swap dye reversals to balance the dyes and samples and to ensure that the resulting data were amenable to statistical analysis.[14] *P*-values as statistical significance measures are accessible through GEO sample numbers GSM84211–GSM84217. Moreover, results were validated by real-time quantitative PCR, which largely confirmed the results for most of the genes tested (Fig. 3).

Transcriptional signature and lung inflammatory cellularity

Consistent with the strong influx of neutrophils in pneumococcal pneumonia, we detected an increase of the relat-

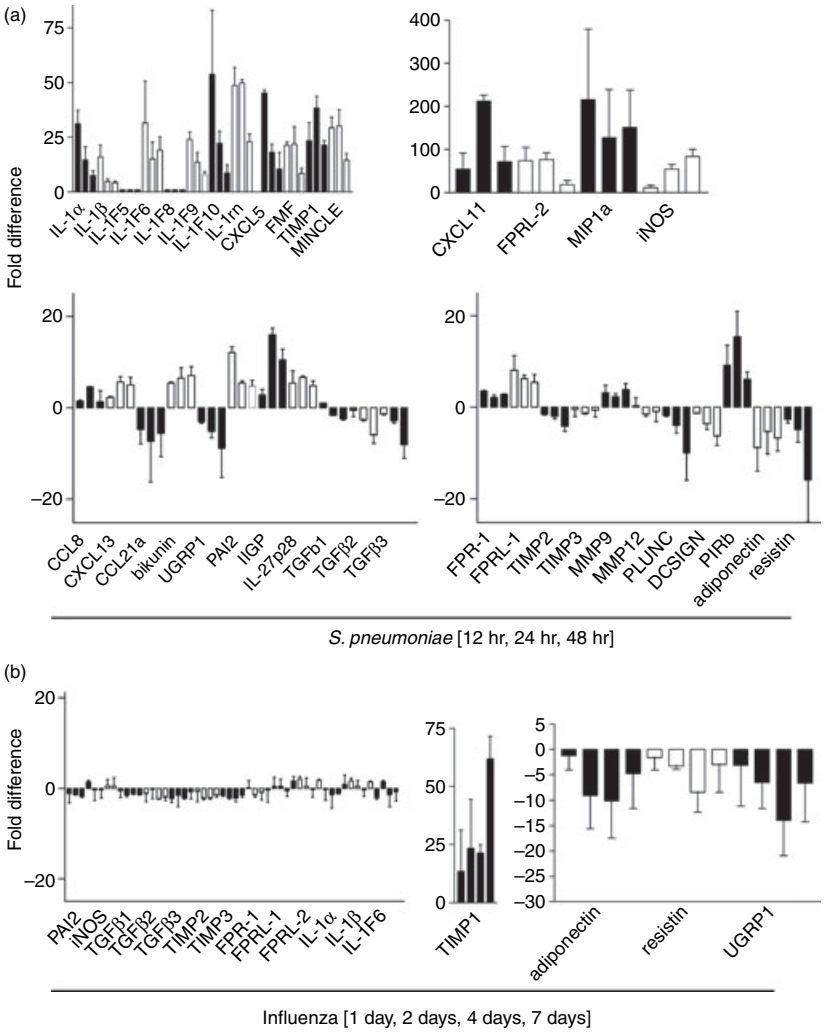

Figure 3. Quantitative PCR analysis of assorted gene products. Real-time quantitative PCR analysis of total lung mRNA from infected and mock-infected mice was performed to verify and extend the microarray data. A positive fold change of gene expression on the *x*-axis reflects increased expression in infected versus control mice and a negative value reflects the opposite. Averaged values from three animals performed in triplicate are depicted. Groups of differentially expressed genes at given time-points after *S. pneumoniae* (a) or influenza A virus infection (b) are shown. Columns of genes depicted in (a) and (b) are shown in a temporally consecutive manner.

ive expression levels of neutrophil-specific genes and of genes implicated in neutrophil function, such as integrin Pactolus-1, Ly6-G, granulocyte colony-stimulating factor (G-CSF), G-CSF receptor, matrix metalloproteinase 9 and tissue inhibitor of metalloproteinase 3. We noted a significant decrease in the expression level of B-cell-specific genes, namely light and heavy immunoglobulin chains, CD19, CD20, CD22, or CD79α/β (Table 1). Further cellular analyses confirmed the disappearance of B cells from the lung, blood, spleen and liver of infected animals (Fig. 4). Influenza infection induced a significant accumulation of virus-specific T cells in the lungs 7 days after virus challenge.[10,12] Accordingly we noted increased relative expression levels of T-cell-specific genes, including CD3δ, CD3γ, CD8α/β, lag-3, osteopontin and CD5 (Table 1).

Orchestration of the pulmonary inflammatory response induced by *S. pneumoniae* and influenza virus

The inflammatory response induced by *S. pneumoniae* is dominated by members of the interleukin-1 (IL-1) family, IL-6 and tumour necrosis factor-a (TNF-α) (Table 2). The participation of IL-1 family members is not only confined to IL-1α and IL-1β; the recently identified members IL-1F6, IL-1F9, and IL-1F10[15] also seem to participate in the pulmonary immune response against this pathogen (Fig. 3; Table 2). A complex balancing of the pro-inflammatory activities is shown by strong expression of the IL-1 receptor antagonist and the inert type-II IL-1 receptor. Similarly, we observed marked expression of the pyrin member marenostrin/familial Mediterranean fever, which is involved in dampening IL-1β processing.[16] In influenza virus infection, IL-6 expression was also significantly increased, but differential expression of TNF-α and IL-1 family members was far less prominent as compared to pneumococcal infection. Further modulatory activities in pneumococcal pneumonia were represented by increased expression of IL-10 which could limit the inflammatory response, as well as IL-22 serving to integrate non-immune cells into the innate defence process.[17] Transcripts of myeloid cell-derived IL-27, a cytokine implicated in T helper type 1 responses,[18] were also elevated upon pneumococcal

Table 1. Differential expression of cell-type-specific genes

Gene product		Accession no.	*S. pneumoniae*			Influenza A virus			
			12 hr	24 hr	48 hr	1 day	2 days	4 days	7 days
T-cell specific antigens									
TCRα	TCRα	U07662	1·3	1·2	− 1·5	1·3	1·7	1·1	3·9
TCRβ	TCRβ	AF012147	1·0	− 1·1	− 1·3	1·4	1·3	1·4	3·3
CD3 antigen δ	CD3δ	NM_013487	1·1	− 1·1	− 1·7	1·8	1·8	− 1·2	4·7
CD3 antigen γ	CD3γ	NM_009850	− 1·0	− 1·3	− 2·3	1·8	1·4	− 1·4	3·9
CD8 antigen β-chain	CD8β	NM_009858	1·1	− 1·5	− 2·2	1·6	1·8	1·6	4·1
CD8 antigen α-chain	CD8α	Y00157	1·2	1·1	− 1·4	1·3	1·8	1·4	5·3
Lymphocyte protein tyrosine kinase	Lck	M12056	1·1	− 1·2	− 1·8	1·5	1·6	1·5	3·2
ζ-chain (TCR)-associated protein kinase	ZAP70	BB204558	1·0	1·0	− 1·6	1·3	1·2	1·5	3·2
CD5	CD5	NM_007650	1·5	− 1·1	− 1·6	1·2	1·3	1·2	3·0
CD28	CD28	NM_007642	1·2	− 1·2	− 1·6	1·3	1·4	1·6	3·2
L-selectin	CD62L	NM_011346	2·5	3·9	3·8	3·8	1·5	1·4	1·1
Neutrophil-specific genes									
Integrin β_2-like	Pactolus-1	NM_008405	2·9	5·1	17·3	1·6	− 1·7	1·1	− 2·4
Lymphocyte antigen 6, locus G	Ly6-G	NM_008531	1·7	3·8	4·5	2·0	2·3	1·6	2·2
Colony-stimulating factor 3 receptor	G-CSFR	NM_007782	2·7	2·7	1·9	1·9	− 1·2	− 1·3	− 1·3
Matrix metalloproteinase 9	MMP9	NM_013599	2·8	2·8	4·5	2·3	− 1·5	1·1	− 1·7
Colony-stimulating factor 3	G-CSF	NM_009971	2·9	3·3	5·4	1·1	1·1	1·5	1·1
Tissue inhibitor of metalloproteinase 3	TIMP3	NM_011595	1·1	1·8	2·4	− 1·0	− 1·1	− 1·1	− 1·2
Secretory leucocyte protease inhibitor	SLP1	NM_011414	4·4	5·3	4·2	− 1·3	1·4	− 1·1	1·0
Formyl peptide receptor 1	FPR1	NM_013521	2·7	1·8	3·1	1·2	− 1·1	− 1·0	1·0
Formyl peptide receptor, related sequence 1	FPRL1	NM_008038	4·4	3·4	7·7	1·5	1·0	1·5	1·1
Formyl peptide receptor, related sequence 2	FPRL2	NM_008039	5·3	5·1	5·7	2·9	1·9	1·3	2·1
B-cell-specific genes									
IgL	IgLC	AV063330	1·1	− 3·2	− 8·4	1·0	1·1	− 1·3	− 2·0
Immunoglobulin B-cell antigen receptor gene	IgKC	L28060	1·2	− 2·1	− 5·2	− 2·0	1·4	1·3	2·2
Immunoglobulin heavy chain 6 (heavy chain of IgM)	IgM	V00820	− 1·3	1·2	− 4·6	− 1·6	− 1·1	− 2·1	− 1·0
Immunoglobulin μ-chain C region	IgM	V00827	− 1·0	− 1·4	− 3·9	− 1·0	− 1·0	− 1·4	− 1·0
Immunoglobulin J chain precursor	Igj	J00544	− 1·1	− 1·0	− 3·3	− 2·0	− 1·6	1·4	1·6
Immunoglobulin-associated β	CD79B	NM_008339	1·2	− 2·3	− 4·8	1·1	− 1·1	− 1·6	− 2·9
Immunoglobulin-associated α	CD79A	NM_007655	− 1·3	− 1·6	− 2·4	− 1·3	− 1·4	1·2	− 1·6
CD19	CD19	NM_009844	1·2	− 1·9	− 3·3	1·2	1·0	− 1·2	− 1·4
CD20	CD20	BE686578	1·1	− 3·0	− 12·0	1·0	− 1·0	− 1·2	− 2·3
Complement receptor 2/CR2	CD21	M35684	1·0	− 1·9	− 3·6	− 1·2	1·1	1·1	− 1·6
CD22	CD22	NM_009845	− 1·0	− 1·7	− 3·1	− 1·1	− 1·0	− 1·1	− 1·4

infection. In addition, we noted increased IL-17 expression, a cytokine involved in the recruitment of neutrophils and considered critical for the combat of acute pulmonary infection.[19,20] Common to both cytokine-orchestrated inflammatory events is an underlying prominent type I and type II interferon (IFN)-mediated response represented by induction of members of the 65 000 or 47 000 molecular weight GTPase gene family (GBP2, GBP4, GTPI, IIGP) and other known IFN-responsive genes including IFI16, IFI35 and PUMA-G[21] (Table 2, Table S2). On the chemokine level, both pathogens induced expression of CCL20, MCP1, IP10, MIG, KC/Gro1, MCP3, RANTES and MIP2/Gro2. The pneumococcal infection was further characterized by MCP5, LIX, MIP1α and MIP1β (Table S2), driving attraction of monocytes/macrophages and neutrophils, as well as IP9/ITAC, which is strongly induced by IFN-γ and is known to attract activated T cells and plasmacytoid dendritic cells.[22] Overall, chemokines implicated in the recruitment of T cells (CCL21a/b) as well as B cells (CXCL13/BCA1, CXCL12) were significantly less expressed compared to influenza infection, which is featured by marked elevation of BCA1, and – at later stages – of CCL1, lymphotactin and CCL8/MCP2 (Table S2).

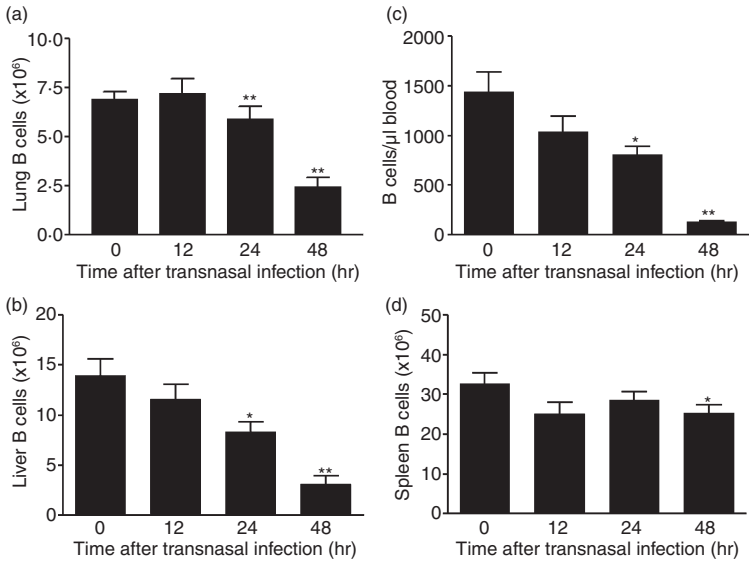

Figure 4. Disappearance of B lymphocytes in pneumococcal pneumonia. Mice transnasally infected with *S. pneumoniae* were killed 12 hr, 24 hr or 48 hr after infection. Control mice were challenged with 20 µl PBS and killed after 48 hr. Lung, liver and spleen cells were counted using a haemocytometer and B cells were further differentiated by FACS analysis of CD45 and CD19 expression. Blood B cells were quantified by FACS using BD Truecount in combination with CD45 and CD19 labelling. Data are presented as mean B-cell numbers ± SEM, $^{*}P < 0{\cdot}05$, $^{**}P < 0{\cdot}01$ versus control, $n = 5$ each experiment.

Table 2. Cytokine-mediated orchestration of the immune response

			S. pneumoniae			Influenza A virus			
Gene product		Accession no.	12 hr	24 hr	48 hr	1 day	2 days	4 days	7 days
Interleukin-1α	IL-1α	NM_010554	12·0	7·3	7·7	2·4	2·1	1·6	− 1·0
Interleukin-1b	IL-1β	NM_008361	11·5	6·6	6·7	3·7	1·1	1·6	− 1·3
Interleukin-1F6	IL-1F6	NM_019450	7·2	6·3	14·2	− 1·8	1·3	− 1·2	2·1
IL-1 receptor antagonist	IL-1RA	BE457883	11·2	10·3	9·5	4·0	2·5	1·4	1·8
Interleukin-6	IL-6	J03783	33·8	24·8	31·0	17·3	19·9	7·2	7·9
Tumour necrosis factor-α	TNFα	NM_013693	5·7	5·9	3·8	1·1	1·2	1·2	1·1
Interleukin-10	IL-10	NM_010548	2·6	2·4	7·7	1·3	1·2	1·1	2·0
Interleukin-17	IL-17	NM_010552	3·8	2·9	2·2	1·1	− 1·1	2·2	− 1·2
Interleukin-22	IL-22	NM_016971	3·6	2·6	1·5	− 1·4	1·2	1·3	1·0
Interleukin-27	IL-27	NM_015766	4·0	4·3	4·8	1·5	1·3	1·5	1·2
Interferon-γ	IFNγ	M28621	4·5	9·8	3·9	3·1	2·0	1·0	6·9
Interferon-β	IFNβ	NM_010510	1·9	2·6	5·5	3·4	5·6	1·8	1·1
Interferon-activated gene 204	IFI204	NM_008329	10·6	25·6	22·4	15·1	12·4	6·7	9·2
Interferon-inducible GTPase	IIGP	AF194871	3·9	23·5	13·1	8·7	7·5	5·6	15·0
Seven transmembrane spanning receptor, Puma-g	PUMA-G	AV249683	11·7	12·3	8·1	3·7	4·6	1·8	1·9

The transcriptional signature common to both infections

Differentially expressed genes shared by the immune responses against both pathogens reflected the activation of lung-resident macrophages (Table 3; Table S2). Various Fc receptor elements, such as FcγRIII, FcεRI, FcγRIa, FcγRIIb, and the macrophage scavenger receptor MSR1 were strongly up-regulated after both infections. Similarly, a group of C-type lectin receptors, which are preferentially expressed in myeloid cells, was strongly induced upon pneumococcal infection and to a lesser degree in response against influenza. These include MPCL, MDL-1 and Mincle.[23–25] In contrast, the uteroglobin-related protein-1, a putative opsonin exclusively expressed in the lung, was strongly down-regulated.[26] Further, we observed elevated expression of genes implicated in anti-inflammatory regulation, such as the Mac-2 binding protein, suppressors of cytokine signalling-1 and -3, FcγRIIb, as well as gp49A and gp49B1, a set of receptors that negatively regulate neutrophils, mast cells and macrophages in an inflammatory environment.[27,28]

The pathogen-specific transcriptional signatures of *S. pneumoniae* and influenza A virus

The sustained elevated expression of most activating paired immunoglobulin-like receptor family members

Table 3. The response common to *S. pneumoniae* and influenza A virus

Gene product		Accession no.	*S. pneumoniae*			Influenza A virus			
			12 hr	24 hr	48 hr	1 day	2 days	4 days	7 days
Fc receptor, IgG, low affinity III	CD16	NM_010188	2·1	2·5	3·0	1·9	1·7	2·0	2·9
Fc receptor, IgE, high affinity I, γ	FCER1G	NM_010185	3·3	4·7	5·4	2·4	2·2	2·2	3·7
Fc receptor, IgG, high affinity I	FCGR1A	NM_010186	3·7	9·0	7·4	10·6	11·5	6·9	8·3
Fc receptor, IgG, low affinity Iib, CD32	FCGR2B	NM_010187	2·4	4·4	9·0	2·3	3·2	2·7	5·0
Scavenger receptor, SCVR	MSR1	AF203781	3·2	5·9	8·5	3·1	6·1	2·1	7·4
Macrophage C-type lectin, Clecsf8	MPCL	NM_010819	15·5	14·1	14·3	4·6	1·9	1·6	1·0
C-type lectin, Clecsf5	MDL-1	NM_021364	3·0	4·4	4·9	2·7	3·8	2·3	4·1
C-type lectin, Clecsf9	MINCLE	NM_019948	38·0	31·0	33·2	7·8	4·7	1·1	2·7
Mac-2-binding protein (M2BP)	PPICAP	NM_011150	1·7	3·6	4·1	3·2	5·6	3·2	4·0
Caspase 1	CASP1	NM_009807	2·3	4·5	3·3	2·6	2·1	2·0	2·8
Caspase 11	CASP11	NM_007609	4·3	6·3	5·4	4·0	3·2	2·4	2·4
Serum amyloid A 3	SAA3	NM_011315	8·8	8·4	4·8	16·0	23·6	14·6	15·3
Uteroglobin-related protein	UGRP1	AV365605	− 1·9	− 2·9	− 3·6	− 1·5	− 4·5	− 6·6	− 7·6
Lecithin retinol acyltransferase	LRAT	BE197763	− 2·1	− 3·1	− 8·7	− 1·3	− 2·3	− 1·5	− 9·7
Uridine phosphorylase	UP	NM_009477	3·5	4·6	4·5	2·5	1·9	1·5	2·8
Purine nucleoside phosphorylase	NP	NM_13632	1·4	3·9	4·3	4·3	2·0	2·5	3·3

(PIRA1-7, -10, -11), including the inhibitory PIRB member,[29] marks pneumococcal pneumonia, which is in stark contrast to the weak and temporary increase induced by influenza infection (Table 4; Table S2). These molecules are preferentially expressed in myeloid cells. Another important receptor family modulating the inflammatory response of myeloid cells comprises the triggering receptors expressed on myeloid cells (TREM).[30] TREM-1 was strongly induced in both infections, which is consistent with its capacity to trigger the secretion of pro-inflammatory chemokines and cytokines in phagocytes. Elevated expression of TREM-2, which activates monocyte-derived dendritic cells, marked the late phase of influenza infection, whereas macrophage expression of TREM-3 was associated with pneumococcal infection. Numerous genes relevant for proper functioning of myeloid cells, including alveolar macrophages, dendritic cells, or recruited monocytes, were specifically elevated after infection with *S. pneumoniae*. These include elements of the toll-like receptors (TLR)/IL-1R-MyD88-NFκB-pathway, e.g. CD14, MyD88, IRAK-3, IKBKε and IκBζ; or the transcription factor Spi-C, implicated in the end-differentiation of myeloid cells; the complement receptor 3 (Mac-1); and various formyl peptide receptors, consistent with the strong neutrophil influx. In contrast, increased expression of TLR1, TLR2, TLR6 and TLR7 proceeded in a pathogen-independent manner. The induction of the TNF-α responsive A20 gene and its interacting protein, the Nef-associated protein NAF1 was specific for pneumococcal infection. Both products seem to be important for limiting TLR-induced TNF-α.[31] Further elements that modulate the severity of inflammation include the lipopolysaccharide detoxifying activity of the neutrophilic acyloxyacyl hydrolase;[32] the anti-apoptotic and inflammation modulatory sphingosine kinase-1; and the nonsignalling Duffy antigen/receptor for chemokines.[33] Protection against reactive oxygen could be attributed to peroxisomal membrane protein 20 (PRDX5) showing increased expression during pneumococcal infection.[34] As expected, the immune response against pneumococci was accompanied by strong prostaglandin synthesis, reflected by COX-2 up-regulation and controlled by MAP3K8, which is important for TNF-α production. The febrile response induced by prostaglandin E_2, is mediated by prostaglandin E receptor 3,[35] which was significantly down-modulated in pneumococcal pneumonia. Along with iNOS induction, we observed elevated levels of type I and type II arginase (Table 4). While both genes were specifically induced upon pneumococcal infection, levels of arginase type-I increased in a pathogen-independent manner. In pneumococcal pneumonia we further detected increased expression of anti-coagulative elements, such as tissue factor pathway inhibitor-2, endothelial protein receptor C and the urokinase plasminogen activator receptor, as well as anti-fibrinolytic enzymes represented by type II monocyte/macrophage-derived plasminogen activator inhibitor and type I plasminogen activator inhibitor (Table S2). Unique responses against influenza virus infection include elevated expression of genes implicated in the regulation of the cell cycle (Table 4; Table S2), as well as increased expression of numerous cytokeratin genes. Despite the important role of the classical complement pathway for protection against *S. pneumoniae*,[36] elements of the complement complex 1 (C1qa/b/c) were exclusively up-regulated during influenza virus infection. We also observed elevated levels of amphiregulin and epiregulin exclusively after influenza infection. Both are members of

Table 4. The pathogen-specific response

Gene product		Accession no.	*S. pneumoniae*			Influenza A virus			
			12 hr	24 hr	48 hr	1 day	2 days	4 days	7 days
Paired Ig-like receptor A4	PIRA4	U96685	3·4	3·7	5·0	2·0	1·6	1·4	1·4
Paired Ig-like receptor A7	PIRA7	U96688	3·1	3·5	5·2	2·1	1·6	1·3	1·4
Paired Ig-like receptor B	PIRB	U96693	2·7	5·0	6·3	2·9	2·0	1·4	2·2
Triggering receptor expressed on monocytes 1	TREM1	NM_021406	8·8	8·6	10·5	6·8	3·5	1·0	2·1
Triggering receptor expressed on myeloid cells 2	TREM2	NM_021410	− 1·0	− 1·0	1·4	1·1	1·4	3·4	3·9
Triggering receptor expressed on monocytes 3	TREM3	NM_021407	4·3	4·3	4·9	2·1	− 1·0	− 1·1	− 1·5
EST, similar to pelle-like protein kinase, IRAK-M	IRAK3	AV367083	3·6	3·2	4·9	1·5	1·5	1·3	1·3
Inducible IκB kinase	IKBKε	NM_019777	3·1	5·3	5·8	1·3	1·6	− 1·0	1·8
EST	IκB-ζ	AI451537	7·1	4·9	4·8	1·5	1·0	1·1	1·3
Spi-C transcription factor	SPI-C	NM_011461	2·2	5·8	11·1	1·3	2·9	1·7	1·6
TBX protein	LITAF	NM_019980	3·3	3·5	4·3	2·0	2·3	1·8	1·9
Nef-associated factor 1, TNFAIP3 interacting protein	NAF1	NM_021327	3·0	3·4	3·9	1·6	1·8	1·8	1·7
Tumor necrosis factor-α-induced protein 3, A20	TNFAIP3	NM_009397	3·3	2·6	2·4	1·1	1·1	− 1·2	1·5
EST, acyloxyacyl hydrolase	AOAH	AV370401	1·1	2·1	2·8	1·1	1·7	1·0	− 1·3
Sphingosine kinase	SPHK1	AF068748	1·9	2·6	7·2	1·7	2·0	1·3	1·9
Chemokine receptor/Duffy blood group	DARC	NM_010045	3·7	2··9	3·6	1·7	1·7	1·4	1·8
Peroxisomal membrane protein 20	PRDX5	NM_012021	1·6	3·1	4·0	1·6	1·4	1·2	1·7
Myeloid differentiation primary response gene 118	GADD45B	NM_008655	5·3	7·3	5·1	1·0	1·5	2·2	1·3
Prostaglandin E receptor 3 (subtype EP3)	PTGER3	NM_011196	− 1·2	− 1·3	− 7·0	− 1·5	− 1·2	− 1·1	− 1·2
Nitric oxide synthase 2, inducible, macrophage	iNOS	NM_010927	1·7	2·5	5·9	2·3	1·1	− 1·2	− 1·0
Arginase type II	ARG2	NM_009705	4·7	7·1	7·7	1·8	1·5	1·1	1·4
Arginase 1, liver	ARG1	NM_007482	1·3	6·3	10·0	1·6	7·5	2·7	16·1
Complement component 1, qα	C1qa	NM_007572	− 1·1	1·7	1·8	1·3	2·9	3·2	5·3
Complement component 1, qβ	C1qb	NM_009777	− 1·2	2·0	2·2	1·3	2·8	3·1	5·2
Complement component 1, qc	C1qc	NM_007574	− 1·3	1·6	1·4	1·1	2·9	3·1	5·5
Amphiregulin	AREG	NM_009704	1·5	− 2·0	1·8	4·6	4·6	10·5	12·3
Trefoil factor 1	TFF1	NM_009362	1·2	1·2	− 1·1	− 1·1	− 1·0	1·0	4·4
Putative cell cycle control protein	SDP35	BE29562	1·2	− 1·1	− 2·3	1·3	1·3	1·6	4·1
Cell division cycle 2	CDC2	NM_007659	− 1·0	− 1·2	− 1·2	1·2	1·3	1·8	3·3
CDC28 protein kinase 1	Cks1	NM_016904	1·0	− 1·0	− 1·2	1·2	1·4	2·0	2·5
Antigen Ki 67	MK167	X82786	1·3	1·3	1·3	1·2	1·3	1·3	3·6
Cyclin B1, r·s·1	CCNB1-rs1	NM_007629	1·2	− 1·2	− 1·6	− 1·3	1·3	1·0	7·8

the EGF gene family, and their involvement in tissue regeneration and wound healing has been suggested.[37] Likewise, the late-stage up-regulated trefoil factor-1, originally described as a stomach-specific gene, is considered relevant to general repair of mucosal epithelia.[38] The extensive degree of tissue destruction after influenza virus infection can be deduced from the relatively strong decrease in the expression of gene products contributing to lung homeostasis, such as surfactant protein-A and Plunc.

Discussion

Our comparative analysis of the pulmonary transcriptional signatures induced by *S. pneumoniae* and influenza A virus infection provides information on the molecular framework underlying pathogenesis and protective immunity in pneumonia. We identified both pathogen-specific and shared transcriptional profiles. The individual signatures seem to reflect the differential nature of the processes caused by these pathogens and the differential quality

and strength of the ensuing immune response. Of discriminative value in the case of pneumococcal pneumonia are:

(1) the absolute decrease of pulmonary B cells during the course of infection;
(2) the prominent and comprehensive involvement of IL-1 family members in the orchestration of the response; and
(3) the differential expression of cytokines, chemokines, and additional regulatory elements involved in fine-tuning of the innate immune response against this pathogen.

The early immune response induced by infection with influenza A virus was less intense compared to that provoked by pneumococci. However, at later stages, signs of extensive cellular proliferation and tissue regeneration, as well as T-cell-associated processes, became apparent. At first sight, both pathogens seem to trigger a similar sequence of defence events; these are typically characterized by prominent production of type I and type II interferons, TNF-α and IL-6, and the recruitment of neutrophils and monocytes, as well as activation of tissue-resident macrophages. Furthermore, complement and natural antibodies are crucial for protective responses against both pathogens.[39,40] Innate immune mechanisms are primarily decisive for the outcome of infection with *S. pneumoniae* and this is underscored by the pronounced response of myeloid cell-associated genes. In contrast, cure of influenza A virus infection strongly depends on the adaptive immune response, in particular the generation of influenza-specific T cells.[2,3,7] This is reflected by the conspicuous T-cell-associated gene response 7 days after influenza infection, coinciding with the appearance of *ex vivo* measurable cytotoxic activity and cytokine production.[10,41] The differential expression levels sensitively traced this pulmonary cellular influx and efflux supporting the reliability of our microarray data.

Unanticipated, but a matter of particular interest, is the finding of a dramatic drop of pulmonary B-cell signals in pneumococcal pneumonia. Since cellular analyses revealed the disappearance of B cells not only in the lung but also in peripheral blood, liver and spleen, a decline of B-cell numbers appears more likely than redistribution of pulmonary B cells into extrapulmonary compartments. This seemed to be specifically related to infection with *S. pneumoniae*, because we did not make analogous observations in pulmonary inflammation elicited by influenza virus, *Chlamydia pneumoniae* or *Mycobacterium tuberculosis* (unpublished data). It is known that B cells, especially marginal zone-B and B1 cells producing natural immunoglobulin M, are crucial for defence against encapsulated bacteria including *S. pneumoniae*.[39,42] Therefore, targeting B cells would be an adequate evasion strategy of pneumococci. Interestingly, further experiments indicated up-regulation of B-cell apoptosis in pneumococcal pneumonia (data not shown). Yet, the extent to which the decline of B-cell numbers reflects a pneumococcal strategy aimed at impairing protective immunity remains to be determined.

Intriguingly, expression levels of some of the recently identified new members of the IL-1 family, IL-1F6, IL-1F9 and IL-1F10 were strongly elevated.[15] IL-1Rp2, a receptor for IL-1F6 and IL-1F9, was also highly up-regulated in the lung. It has been suggested that these IL-1 family members constitute an IL-1β-independent, nuclear factor κB signalling system in epithelial cells.[43] Future studies have to clarify whether these newly identified IL-1 family members participate in pneumococcal defence or solely augment the inflammatory response leading to sepsis. In either case, the complex cascade elicited by IL-1 family members stimulated strong expression of a variety of genes implicated in inflammation, including COX-2, type 2 phospholipase A and inducible nitric oxide synthase (iNOS), accounting for large amounts of prostaglandin E_2, platelet-activating factor and nitric oxide, respectively. As represented by sepsis or acute respiratory distress syndrome, uncontrolled inflammatory processes generate cytotoxic activities, resulting in severe tissue damage. Thus, a multitude of regulatory elements are necessary to sustain an appropriate balance of beneficial and detrimental inflammatory sequels during the immune response. Our data emphasize the overall complexity of the processes involved, because many differentially expressed gene products participate in anti-inflammatory regulatory circuits. Obviously, this reflects the enduring need for a local balance between effective immune protection and collateral damage.

We observed selective up-regulation of the PIRs after pneumococcal infection, but not after influenza virus infection. PIRs are part of a signalling system that exerts a modulatory role in inflammation.[29] The activating PIR-A family members, mainly expressed on myeloid cells, could be involved in fine-tuning of the activation state and functionality of the pulmonary monocyte/macrophage response. The TREM receptors comprise another protein family implicated in the modulation of haematopoietic cells awaiting detailed characterization.[30] Known as amplifiers of inflammation in neutrophils and macrophages, the prognostic value of TREM-1 expression in sepsis and pneumonia is currently being discussed.[44,45] Putative detrimental consequences are also associated with increased expression of the immunomodulatory platelet-activating factor receptor, which contributes not only to the regulation of inflammation, but also facilitates pneumococcal invasion and dissemination.[46] Likewise, the IFN-γ-mediated induction of the polymeric immunoglobulin receptor, expressed on lung epithelial cells, potentially facilitates invasion of pneumococci.[47] Increasing

evidence suggests that influenza infection promotes adherence and invasion of pneumococci by the up-regulation of these molecules, reflecting one of the multiple mechanisms triggering severe and often fatal pneumococcal pneumonia in pandemic influenza.[4]

Coagulopathy is a hallmark of sepsis, and therapies for septic patients specifically target this pathway.[48] Disturbances in coagulation and fibrinolysis have also been demonstrated in patients with pneumonia,[49] implying novel therapeutic or preventive intervention strategies. Here, we present evidence for considerable modification of the pulmonary coagulation cascade in the course of pneumococcal pneumonia. Notably, *S. pneumoniae* induced increased expression of anti-coagulative elements in the lung. Up-reguation of fibrinolytic enzymes is somewhat surprising, but actual impairment of fibrinolysis and hence predominance of pro-coagulant pathways might be reflected by increased expression of several plasminogen activator inhibitors.

Altogether, our approach contributes to the elucidation of molecular inflammatory processes in the lung elicited by two of the most important pathogens responsible for community-acquired pneumonia. The identification of common signatures as well as unique differences in gene expression profiles can provide useful information about suitable targets for novel intervention strategies, particularly with regard to the mechanisms responsible for the menacing synergism between influenza virus and *S. pneumoniae*.

Acknowledgements

We are grateful to Sandra Leitner, Karin Hahnke and Kathrin Wricke for technical assistance and cellular analyses. The influenza HKx31 virus stock was kindly provided by Dr Thomas Wolff (Robert Koch Institute, Berlin, Germany). We especially thank Dr Kerstin Bonhagen (Friedrich-Schiller-Universität Jena, Germany) for help with the influenza infections and Dr Sven Hammerschmidt (University of Würzburg, Germany) for providing *S. pneumoniae* serotype 3. This work was supported in part by grants from the German Federal Ministry of Education and Research to J.Z. and S.H.E.K. (grant BMBF-Capnetz C2), S.R. and N.S. (grant BMBF-Capnetz C4) and to H.J.M. and S.H.E.K. (grant ERDF/State of Berlin (WF-3102/10020681).

References

1 File TM. Community-acquired pneumonia. *Lancet* 2003; **362**:1991–2001.
2 Shorr AF. Preventing pneumonia: the role for pneumococcal and influenza vaccines. *Clin Chest Med* 2005; **26**:123–34.
3 Oliveira EC, Lee B, Colice GL. Influenza in the intensive care unit. *J Intensive Care Med* 2003; **18**:80–91.
4 McCullers JA. Insights into the interaction between influenza virus and pneumococcus. *Clin Microbiol Rev* 2006; **19**:571–82.
5 Novak R, Tuomanen E. Pathogenesis of pneumococcal pneumonia. *Semin Respir Infect* 1999; **14**:209–17.
6 Kadioglu A, Andrew PW. The innate immune response to pneumococcal lung infection: the untold story. *Trends Immunol* 2004; **25**:143–9.
7 Lipatov AS, Govorkova EA, Webby RJ, Ozaki H, Peiris M, Guan Y, Poon L, Webster RG. Influenza: emergence and control. *J Virol* 2004; **78**:8951–9.
8 Kash JC, Basler CF, Garcia-Sastre A *et al.* Global host immune response: pathogenesis and transcriptional profiling of type A influenza viruses expressing the hemagglutinin and neuraminidase genes from the 1918 pandemic virus. *J Virol* 2004; **78**:9499–511.
9 Schmeck B, Zahlten J, Moog K *et al. Streptococcus pneumoniae*-induced p38 MAPK-dependent phosphorylation of RelA at the interleukin-8 promotor. *J Biol Chem* 2004; **279**:53241–7.
10 Debes GF, Bonhagen K, Wolff T, Kretschmer U, Krautwald S, Kamradt T, Hamann A. CC chemokine receptor 7 expression by effector/memory CD4+ T cells depends on antigen specificity and tissue localization during influenza A virus infection. *J Virol* 2004; **78**:7528–35.
11 Kadioglu A, Gingles NA, Grattan K, Kerr A, Mitchell TJ, Andrew PW. Host cellular immune response to pneumococcal lung infection in mice. *Infect Immun* 2000; **68**:492–501.
12 Liang S, Mozdzanowska K, Palladino G, Gerhard W. Heterosubtypic immunity to influenza type A virus in mice. Effector mechanisms and their longevity. *J Immunol* 1994; **152**:1653–61.
13 Schmitz N, Kurrer M, Bachmann MF, Kopf M. Interleukin-1 is responsible for acute lung immunopathology but increases survival of respiratory influenza virus infection. *J Virol* 2005; **79**:6441–8.
14 Churchill GA. Fundamentals of experimental design for cDNA microarrays. *Nat Genet* 2002; **32** (Suppl.):490–5.
15 Taylor SL, Renshaw BR, Garka KE, Smith DE, Sims JE. Genomic organization of the interleukin-1 locus. *Genomics* 2002; **79**:726–33.
16 Chae JJ, Komarow HD, Cheng J, Wood G, Raben N, Liu PP, Kastner DL. Targeted disruption of pyrin, the FMF protein, causes heightened sensitivity to endotoxin and a defect in macrophage apoptosis. *Mol Cell* 2003; **11**:591–604.
17 Wolk K, Kunz S, Witte E, Friedrich M, Asadullah K, Sabat R. IL-22 increases the innate immunity of tissues. *Immunity* 2004; **21**:241–54.
18 Villarino AV, Huang E, Hunter CA. Understanding the pro- and anti-inflammatory properties of IL-27. *J Immunol* 2004; **173**:715–20.
19 Linden A, Adachi M. Neutrophilic airway inflammation and IL-17. *Allergy* 2002; **57**:769–75.
20 Ruddy MJ, Shen F, Smith JB, Sharma A, Gaffen SL. Interleukin-17 regulates expression of the CXC chemokine LIX/CXCL5 in osteoblasts: implications for inflammation and neutrophil recruitment. *J Leukoc Biol* 2004; **76**:135–44.
21 Boehm U, Klamp T, Groot M, Howard JC. Cellular responses to interferon-gamma. *Annu Rev Immunol* 1997; **15**:749–95.
22 Vanbervliet B, Bendriss-Vermare N, Massacrier C, Homey B, de Bouteiller O, Briere F, Trinchieri G, Caux C. The inducible CXCR3 ligands control plasmacytoid dendritic cell responsive-

ness to the constitutive chemokine stromal cell-derived factor 1 (SDF-1)/CXCL12. *J Exp Med* 2003; **198**:823–30.
23 Balch SG, Greaves DR, Gordon S, McKnight AJ. Organization of the mouse macrophage C-type lectin (Mcl) gene and identification of a subgroup of related lectin molecules. *Eur J Immunogenet* 2002; **29**:61–4.
24 Flornes LM, Bryceson YT, Spurkland A, Lorentzen JC, Dissen E, Fossum S. Identification of lectin-like receptors expressed by antigen presenting cells and neutrophils and their mapping to a novel gene complex. *Immunogenetics* 2004; **56**:506–17.
25 Arce I, Martinez-Munoz L, Roda-Navarro P, Fernandez-Ruiz E. The human C-type lectin CLECSF8 is a novel monocyte/macrophage endocytic receptor. *Eur J Immunol* 2004; **34**:210–20.
26 Bin LH, Nielson LD, Liu X, Mason RJ, Shu HB. Identification of uteroglobin-related protein 1 and macrophage scavenger receptor with collagenous structure as a lung-specific ligand–receptor pair. *J Immunol* 2003; **171**:924–30.
27 Zhou JS, Friend DS, Feldweg AM, Daheshia M, Li L, Austen KF, Katz HR. Prevention of lipopolysaccharide-induced microangiopathy by gp49B1: evidence for an important role for gp49B1 expression on neutrophils. *J Exp Med* 2003; **198**:1243–51.
28 Lee KM, McNerney ME, Stepp SE, Mathew PA, Schatzle JD, Bennett M, Kumar V. 2B4 acts as a non-major histocompatibility complex binding inhibitory receptor on mouse natural killer cells. *J Exp Med* 2004; **199**:1245–54.
29 Takai T, Ono M. Activating and inhibitory nature of the murine paired immunoglobulin-like receptor family. *Immunol Rev* 2001; **181**:215–22.
30 Colonna M. TREMs in the immune system and beyond. *Nat Rev Immunol* 2003; **3**:445–53.
31 Boone DL, Turer EE, Lee EG *et al.* The ubiquitin-modifying enzyme A20 is required for termination of Toll-like receptor responses. *Nat Immunol* 2004; **5**:1052–60.
32 Munford RS, Hunter JP. Acyloxyacyl hydrolase, a leukocyte enzyme that deacylates bacterial lipopolysaccharides, has phospholipase, lysophospholipase, diacylglycerollipase, and acyltransferase activities *in vitro*. *J Biol Chem* 1992; **267**:10116–21.
33 Dawson TC, Lentsch AB, Wang Z, Cowhig JE, Rot A, Maeda N, Peiper SC. Exaggerated response to endotoxin in mice lacking the Duffy antigen/receptor for chemokines (DARC). *Blood* 2000; **96**:1681–4.
34 Fujii J, Ikeda Y. Advances in our understanding of peroxiredoxin, a multifunctional, mammalian redox protein. *Redox Rep* 2002; **7**:123–30.
35 Ushikubi F, Segi E, Sugimoto Y *et al.* Impaired febrile response in mice lacking the prostaglandin E receptor subtype EP3. *Nature* 1998; **395**:281–4.
36 Brown JS, Hussell T, Gilliland SM, Holden DW, Paton JC, Ehrenstein MR, Walport MJ, Botto M. The classical pathway is the dominant complement pathway required for innate immunity to *Streptococcus pneumoniae* infection in mice. *Proc Natl Acad Sci USA* 2002; **99**:16969–74.
37 Hashimoto K. Regulation of keratinocyte function by growth factors. *J Dermatol Sci* 2000; **24**:S46–50.
38 Taupin D, Podolsky DK. Trefoil factors: initiators of mucosal healing. *Nat Rev Mol Cell Biol* 2003; **4**:721–32.
39 Kruetzmann S, Rosado MM, Weber H *et al.* Human immunoglobulin M memory B cells controlling *Streptococcus pneumoniae* infections are generated in the spleen. *J Exp Med* 2003; **197**:939–45.
40 Baumgarth N, Chen J, Herman OC, Jager GC, Herzenberg LA. The role of B-1 and B-2 cells in immune protection from influenza virus infection. *Curr Top Microbiol Immunol* 2000; **252**:163–9.
41 Kretschmer U, Bonhagen K, Debes GF *et al.* Expression of selectin ligands on murine effector and IL-10-producing CD4(+) T cells from non-infected and infected tissues. *Eur J Immunol* 2004; **34**:3070–81.
42 Carsetti R, Rosado MM, Donnanno S *et al.* The loss of IgM memory B cells correlates with clinical disease in common variable immunodeficiency. *J Allergy Clin Immunol* 2005; **115**:412–17.
43 Towne JE, Garka KE, Renshaw BR, Virca GD, Sims JE. Interleukin (IL) -1F6, IL-1F8, and IL-1F9 signal through IL-1Rrp2 and IL-1RAcP to activate the pathway leading to NF-kappaB and MAPKs. *J Biol Chem* 2004; **279**:13677–88.
44 Gibot S, Kolopp-Sarda MN, Bene MC, Cravoisy A, Levy B, Faure GC, Bollaert PE. Plasma level of a triggering receptor expressed on myeloid cells. 1: Its diagnostic accuracy in patients with suspected sepsis. *Ann Intern Med* 2004; **141**:9–15.
45 Richeldi L, Mariani M, Losi M *et al.* Triggering receptor expressed on myeloid cells: role in the diagnosis of lung infections. *Eur Respir J* 2004; **24**:247–50.
46 Rijneveld AW, Weijer S, Florquin S, Speelman P, Shimizu T, Ishii S, van der Poll T. Improved host defense against pneumococcal pneumonia in platelet-activating factor receptor-deficient mice. *J Infect Dis* 2004; **189**:711–16.
47 Kaetzel CS. Polymeric Ig receptor: defender of the fort or Trojan horse? *Curr Biol* 2001; **11**:R35–8.
48 van der Poll T. Coagulation and inflammation. *J Endotoxin Res* 2001; **7**:301–4.
49 Gunther A, Mosavi P, Heinemann S *et al.* Alveolar fibrin formation caused by enhanced procoagulant and depressed fibrinolytic capacities in severe pneumonia. Comparison with the acute respiratory distress syndrome. *Am J Respir Crit Care Med* 2000; **161**:454–62.

Supplementary Material

The following supplementary material is available for this article online:

Table S1.

Table S2.

This material is available as part of the online article from http://www.blackwell-synergy.com